Cardiovascular Research (2009) **84**, 416–424
doi:10.1093/cvr/cvp237

NF-κB activation is required for adaptive cardiac hypertrophy

Laura Zelarayan[1,2], Anke Renger[1,2], Claudia Noack[1,2], Maria-Patapia Zafiriou[1,2], Christina Gehrke[1,2], Roel van der Nagel[3], Rainer Dietz[1,2], Leon de Windt[3], and Martin W. Bergmann[1,2]*

[1]*Department of Cardiology, Franz Volhard Klinik, Experimental Clinical Research Center (ECRC), Charité Campus Buch, Berlin, Germany;* [2]*Max Delbrück Center for Molecular Medicine, Berlin, Germany; and* [3]*Division of Heart and Lungs, Department of Medical Physiology, University Medical Center Utrecht, Utrecht, The Netherlands*

Received 25 November 2008; revised 29 June 2009; accepted 8 July 2009; online publish-ahead-of-print 20 July 2009

Time for primary review: 27 days

KEYWORDS
NF-κB;
Hypertrophy;
Remodelling;
Signal transduction;
Apoptosis;
Fibrosis;
Angiotensin;
Hypertension

Aims We have previously shown that cardiac-specific inhibition of NF-κB attenuates angiotensin II (AngII)-induced left ventricular (LV) hypertrophy *in vivo*. We now tested whether NF-κB inhibition is able to block LV remodelling upon chronic pressure overload and chronic AngII stimulation.
Methods and results Cardiac-restricted NF-κB inhibition was achieved by expression of a stabilized IκBα mutant (IκBαΔN) in cells with an active α-myosin heavy chain (αMHC) promoter employing the Cre/lox technique. Upon low-gradient trans-aortic constriction (TAC, gradient 21 ± 3 mmHg), hypertrophy was induced in both male and female control mice after 4 weeks. At this time, LV hypertrophy was blocked in transgenic (TG) male but not female mice with NF-κB inhibition. Amelioration of LV hypertrophy was associated with activation of NF-κB by dihydrotestosterone in isolated neonatal cardiomyocytes. LV remodelling was not attenuated by NF-κB inhibition after 8 weeks TAC, demonstrated by decreased fractional shortening (FS) in both control and TG mice irrespective of gender. Similar results were obtained when TAC was performed with higher gradients (48 ± 4 mmHg). In TG mice, FS dropped to similar low levels over the same time course [FS sham, 29 ± 1% (mean ± SEM); FS control + 14 days TAC, 13 ± 3%; FS TG + 14 days TAC, 9 ± 5%]. Similarly, LV remodelling was accelerated by NF-κB inhibition in an AngII-dependent genetic heart failure model (AT1-R$^{\alpha MHC}$) associated with significantly increased cardiac fibrosis in double AT1-R$^{\alpha MHC}$/TG mice.
Conclusion NF-κB inhibition attenuates cardiac hypertrophy in a gender-specific manner but does not alter the course of stress-induced LV remodelling, indicating NF-κB to be required for adaptive cardiac hypertrophy.

1. Introduction

Arterial hypertension leading to chronic pressure overload triggers a process summarized as left ventricular (LV) remodelling, which aims to maintain cardiac function despite continuous stress. Typically, the heart increases in weight due to increased muscle mass, a process termed cardiac hypertrophy. If pressure overload persists, systolic function declines and the heart dilates. Inhibiting cardiac hypertrophy has emerged as a primary target for new therapeutic approaches in preventing hypertension-induced end-organ damage.[1] More specifically, signalling cascades of mal-adaptive hypertrophy leading to decreased systolic function are regarded as potentially new treatment targets. Conversely, signalling pathways mediating adaptive hypertrophy which stabilizes LV function should be amplified.[2]

At the cellular level a more stringent definition of 'cardiac hypertrophy' refers to the re-expression of foetal cardiac genes and increased cross-sectional area of adult cardiomyocytes. No clear picture has so far emerged that identifies pathways involved in adaptive vs. mal-adaptive hypertrophy. Several mouse models have been generated to study this process specifically targeting αMHC^{pos} cardiomyocytes employing the Cre/lox technique. Generally, αMHC^{pos} cardiomyocytes were shown to undergo cellular hypertrophy, apoptosis, and recently also regeneration; however, the extent of the latter process is very much under debate. Ignoring all the events that take place in cardiac hypertrophy regarding non-αMHC^{pos} cells (inflammation, metalloproteinase activation, and fibrosis) and focusing on the αMHC^{pos} cardiomyocytes, the balance between hypertrophy and apoptosis appears to be critical for global LV remodelling.

* Corresponding author: Department of Cardiology, Asklepios Clinic St Georg, Hanseatic Heart Center, Lohmühlenstr. 5, 20099 Hamburg, Germany. Tel: +49 40 181885 2450; fax: +49 40 181885 4444.
E-mail address: docbergmann@mac.com

Multiple signalling cascades controlling cardiomyocyte growth as well as survival factors converge at a limited number of nuclear transcription factors and their epigenetic control factors; among these, NF-κB integrates calcium-independent signalling pathways. We have previously shown that cardiac-specific, genetic NF-κB inhibition attenuates angiotensin II (AngII)-induced hypertrophy in association with altered expression of the IL6 receptor protein gp130.[3] During the 14-day period of AngII stimulation, no decline in cardiac systolic function was observed; therefore, this study did not allow us to assess the role of NF-κB in cardiac remodelling.

The extent of cardiac hypertrophy following pressure overload is affected by gender. Females respond to the same stimulus with less cardiac remodelling and increased compensatory capacity both in epidemiological studies and experimental models.[4,5] Some studies suggest a role for the oestrogen receptor β. In addition, androgens might drive this process since they positively control cardiac ACE expression, thereby increasing tissue-specific angiotensin levels.[6] However, the signalling pathways and cellular effectors controlling gender-specific aspects of cardiac hypertrophy require further investigation.

Here, we used a ΔN^{MHC} transgenic (TG) mice containing one copy of the NF-κB super-repressor IκBαΔN under the control of the αMHC promoter resulting in inhibition of NF-κB activity.[7,8] The effect of NF-κB inhibition on pressure overload-induced hypertrophy as well as a genetic heart failure model induced by cardiac-restricted overexpression of the angiotensin type I receptor (AT1-R) was investigated. The effect of NF-κB inhibition on cardiac hypertrophy was found to be gender-dependent, since only hypertrophy of male mice was sensitive to NF-κB inhibition. Neither pressure overload nor AT1-R-induced cardiac remodelling was attenuated by NF-κB inhibition. Consistent with our previous results, NF-κB inhibition attenuates cardiac hypertrophy also after chronic pressure overload and AT1-R overexpression. NF-κB inhibition, however, does not prevent cardiac remodelling leading to decreased cardiac function. NF-κB activation therefore contributes to adaptive cardiac hypertrophy.

2. Methods

2.1 Transgenic mice

Generation of heart-specific $c^{loxPI\kappa B\alpha\Delta N}$ mice has been described before.[7,8] Mice expressing Cre-recombinase under the control of the cardiomyocyte-specific α-myosin heavy chain (αMHC) promoter (αMHC-Cre mice) were a generous gift from Dr Michael D. Schneider. AT1-$R^{\alpha MHC}$ mice were provided by M. Nemer and P. Paradis.[9] All mice were bred on a C57Bl/6 background. Littermates negative for either Cre or loxP site were used as controls. All the procedures involving animals were approved by the Berlin animal review board (Reg. 0135/01 and Reg. 0338/05). The investigation conforms with the Guide for the Care and Use of Laboratory Animals published by the US National Institutes of Health (NIH Publication No. 85-23, revised 1996), which has been adopted as a general policy of the Max Delbrück Center.

2.2 Trans-aortic constriction

Chronic pressure overload was induced by constricting the thoracic aorta of male and female mice at 12–16 weeks of age. Banding of the aorta was induced upon anaesthesia (2.4% isoflurane). A 7-0 prolene suture (Ethicon) ligature was pulled around the aorta and either a blunted 25 (low gradient) or 27 G (high gradient) needle was tied. The needle was then removed as described before.[10] Trans-aortic constriction (TAC) was confirmed by echocardiographic analysis and measurement of the flow gradient via CW Doppler. Eight (in the low-gradient model with 25 G needle) or 2 weeks (in the high-gradient model with the 27 G needle) after surgery, mice were sacrificed and hearts were removed for further examination.

2.3 Echocardiography

For the low-gradient model, echocardiography was performed on an Accuson Sequoia (Siemens) instrument equipped with a 13 MHz microprobe scanning head. For the high-gradient model, echocardiography was performed on a VisualSonics Vevo 770 instrument equipped with a 30 MHz scanning head. For echocardiography, mice were anaesthetized by isoflurane inhalation (2% isoflurane). Ventricular measurements were taken before and 2 (high gradient) or 4 and 8 weeks (low gradient) after TAC with three or more readings per mouse. The observer was unaware of the genotypes and treatments.

2.4 RNA quantification

Total RNA from mouse heart tissue was isolated with the RNeasy kit (Qiagen) and cDNA was synthesized with Superscript II reverse transcriptase (RT) (Invitrogen). cDNA was subjected to real-time PCR by SYBR Green Analysis (Qiagen) on an iCycler instrument (Bio-Rad). All real-time PCR sample reactions were performed in triplicates and normalized to GAPDH mRNA expression as described before.[11] A standard curve was created by sequential dilution of the amplified fragment in order to calculate the RNA copy number.

2.5 Histology

For histological analysis, hearts were stained with Masson Trichrome and TUNEL assay as described before.[11]

2.6 Image and data analysis

Microscopic images were captured with a digital microscope (IX70, Olympus). A semi-automated immunofluorescence quantification software (Axiovisions, Zeiss) was used for cross-sectional area measurements in WGA-FITC-stained sections. For measuring the grade of fibrosis, images were taken with a binocular (Stemi 2000, Zeiss) and analysed using ImageJ software.

Results are given as means ± standard errors of the mean. Statistical analysis was performed using ANOVA tests followed by *post hoc* analysis employing the Bonferroni tests using GraphPad Prism version 4. *P*-values <0.05 were considered significant.

3. Results

3.1 Cardiomyocyte-specific NF-κB inhibition in mice

Heart-restricted NF-κB inhibition was achieved employing the Cre/loxP system as described before.[7] Heterozygous mice $I\kappa B\alpha\Delta N^{floxed/+}$ (ΔNloxP) were bred with αMHC-Cre (Cre^{MHC}) TG mice to generate mice with cardiomyocyte-restricted IκBαΔN expression, named ΔN^{MHC}. The NF-κB repressor IκBαΔN, preceded by a stop codon flanked by loxP sites, is integrated in frame into the β-catenin locus replacing exons 3–6. IκBαΔN lacks the destruction box and therefore acts as a super-repressor of NF-κB.[12] Confirmation of heart-restricted IκBαΔN expression by western blot as well as immunostaining of inhibited nuclear translocation of NF-κB subunit p65 in TNF-α-stimulated cardiomyocytes was demonstrated before. ΔN^{MHC} mice exhibit no basal phenotype regarding LV wall dimensions, histology, or echo parameters.[7]

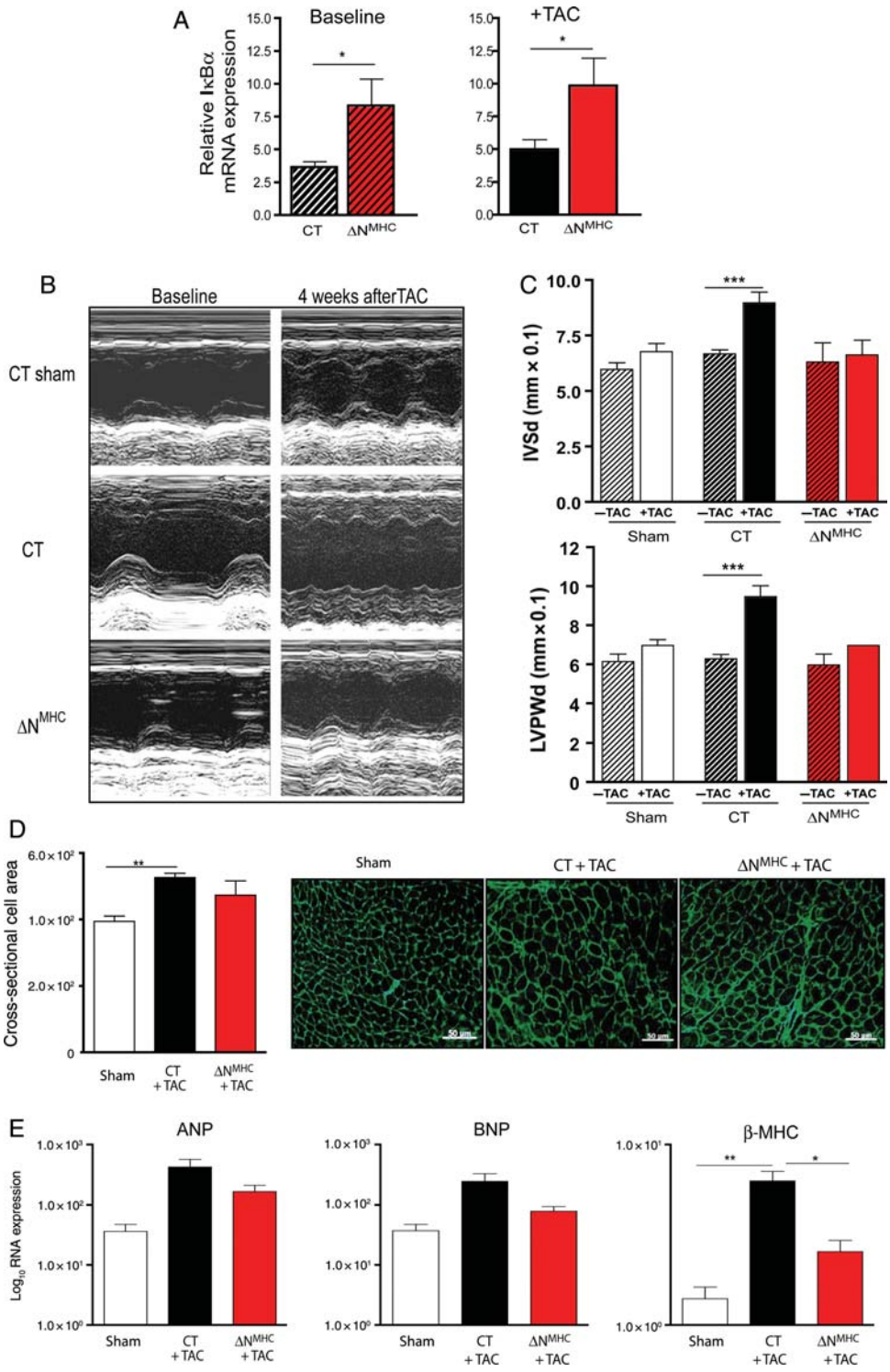

Figure 1 Attenuated LV hypertrophy upon TAC in ΔN^{MHC} mice. (*A*) RNA quantification by real-time RT–PCR analysis of the NF-κB repressor IκBα in ΔN^{MHC} showing significant up-regulation of IκBα in ΔN^{MHC} vs. control mice at baseline and after TAC. (*B*) Representative examples of M-mode echocardiograms of hearts from sham-operated control animals, control, and ΔN^{MHC} mice at baseline and 4 weeks after low-gradient TAC (25 G needle, 21 ± 3 mmHg pressure gradient). TAC increased IVSd and LVPWd in control but not in ΔN^{MHC} mice. (*C*) Quantification of IVSd and LVPWd before and after TAC by echocardiography. $^{**}P < 0.01$, $^{***}P < 0.001$, $n \geq 3$. (*D*) Cross-sectional area analysis by WGA-FITC staining demonstrates a significant increase in cell size in control mice after TAC but no significant change in ΔN^{MHC} mice (scale bar = 50 μm). Quantification is shown (right bar graph). $n = 4$–7 mice per group. (*E*) RNA quantification by real-time RT–PCR analysis of hypertrophic markers in sham, control, and ΔN^{MHC} mice following TAC. A significant difference concerning β-MHC expression following TAC was detected upon NF-κB inhibition. $^{*}P < 0.05$, $^{**}P < 0.01$; expression fold is relative to GAPDH control.

3.2 NF-κB inhibition attenuates TAC-induced hypertrophy

The effect of NF-κB inhibition on LV remodelling was first studied in a model of chronic pressure overload by TAC with low gradient (21 ± 3 mmHg). To validate the experimental model, the overexpression of the repressor IκBα was analysed by quantitative real-time (QRT)-PCR. As expected, expression of IκBα was significantly up-regulated in ΔN^{MHC}

Table 1 Echocardiography M-mode quantification for ΔN^{MHC} mice at baseline and following TAC with low gradient

TAC with low gradient	Sham		Control + TAC		ΔN^{MHC} + TAC	
	Male	Female	Male	Female	Male	Female
IVSd (mm × 0.1)						
Before TAC	6.00 ± 0.32	5.50 ± 0.50	6.71 ± 0.18	6.17 ± 0.17	6.33 ± 0.88	6.14 ± 0.34
4 weeks after TAC	6.80 ± 0.37	6.00 ± 1.00	9.00 ± 0.48*	7.83 ± 0.48*	6.67 ± 0.67§	7.43 ± 0.30
8 weeks after TAC	6.20 ± 0.37	7.50 ± 0.50	8.14 ± 0.40	6.67 ± 0.33	7.00 ± 0.58	6.71 ± 0.29
LVPWd (mm × 0.1)						
Before TAC	6.20 ± 0.37	6.50 ± 0.50	6.43 ± 0.21	6.34 ± 0.21	6.00 ± 0.58	6.86 ± 0.14
4 weeks after TAC	7.00 ± 0.32	7.00 ± 0.00	9.57 ± 0.56*	8.50 ± 0.67*	7.00 ± 0.00§	7.57 ± 0.37
8 weeks after TAC	6.80 ± 0.37	6.50 ± 0.50	8.00 ± 0.58	6.83 ± 0.54	7.33 ± 0.33	7.00 ± 0.49
LVDd (mm)						
Before TAC	3.60 ± 0.21	3.50 ± 0.40	4.00 ± 0.17	3.58 ± 0.11	3.53 ± 0.07	3.24 ± 0.10
4 weeks after TAC	4.04 ± 0.18	3.60 ± 0.30	4.37 ± 0.37	3.88 ± 0.18	4.30 ± 0.38	3.91 ± 0.20
8 weeks after TAC	4.22 ± 0.17	3.75 ± 0.55	5.20 ± 0.35*	4.28 ± 0.23	4.73 ± 0.29	4.06 ± 0.11
FS (%)						
Before TAC	39.1 ± 3.4	46.2 ± 0.2	36.6 ± 3.0	33.9 ± 0.9	35.5 ± 1.3	37.6 ± 2.0
4 weeks after TAC	30.6 ± 1.3	37.9 ± 0.9	33.7 ± 4.0	33.7 ± 3.1	30.2 ± 2.3	36.0 ± 5.5
8 weeks after TAC	30.2 ± 1.5	36.1 ± 2.0	27.2 ± 4.1*	27.5 ± 3.1*	26.3 ± 2.9*	27.2 ± 1.8*
HW/BW (mg/g)	4.4 ± 0.18	4.1 ± 0.31	5.9 ± 0.53*	6.1 ± 0.37*	5.0 ± 0.09	5.3 ± 0.17

Data calculated from M-mode of echocardiograms (measurements in mm in diastole) from both control and TG animals prior to and following TAC with low gradient (25 G needle). IVSd, inter ventricular septum; LVDd, left ventricular diameter; LVPWd, left ventricle posterior wall dimensions; FS, fractional shortening (%); HW/BW, heart weight/body weight at time of sacrifice. *P*-values are given after the two conditions that were compared. Columns with comparative asterisks are compared with the appropriate data of sham mice (*$P < 0.05$). Columns with § are significant to control mice + TAC ($^{§}P < 0.05$). $n = 5$–11 for each experiment.

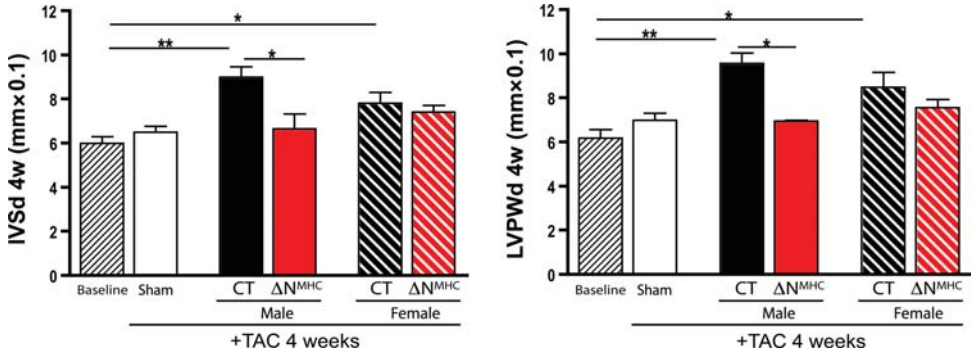

Figure 2 Specific role of NF-κB in cardiac hypertrophy of male mice. Gender-specific analysis of IVSd and LVPWd in control and ΔN^{MHC} mice. A significant attenuation of cardiac hypertrophy as measured by echocardiographic IVSd and LVPWd diameters is observed only in TG male mice. *$P < 0.05$, **$P < 0.01$; $n = 3$–7 mice per group.

mice at baseline and 4 weeks after TAC in comparison to the control littermates (including wild-type, Cre^{MHC}, and ΔNloxP mice) (*Figure 1A*), indicating efficient αMHC-dependent Cre recombination events even upon variation of αMHC expression under cardiac hypertrophy. Next, ΔN^{MHC} mice and controls were analysed by echocardiography 4 weeks following low-gradient TAC. Consistent with our previous results, ΔN^{MHC} mice exhibited an attenuation of cardiac hypertrophy in comparison to control mice that showed significantly increased diameters of diastolic interventricular septum (IVSd) (control baseline: 6.33 ± 0.88 vs. control + TAC: 9.0 ± 0.49 mm × 0.1, $P < 0.01$ and ΔN^{MHC} baseline: 6.71 ± 0.18 vs. ΔN^{MHC} + TAC: 6.67 ± 0.67 mm × 0.1) and LV posterior wall dimensions (LVPWd) (control baseline: 6.33 ± 0.21 vs. control ± TAC: 9.5 ± 0.56 mm × 0.1 and ΔN^{MHC} baseline: 6.00 ± 0.58 vs. ΔN^{MHC} ± TAC: 7.00 ± 0.00 mm × 0.1) (*Figure 1B* and *C*, and *Table 1*). Cardiac hypertrophy was further confirmed by cross-sectional area analysis in control mice after TAC, in which cell area average of control mice ($5.3 \times 102 \pm 0.13 \times 102\ \mu m^2$) increased significantly in comparison to the cell size of sham-operated mice ($3.9 \times 102 \pm 0.16 \times 102\ \mu m^2$, $P < 0.01$) (*Figure 1D*), whereas no significant changes were observed in ΔN^{MHC} mice. Moreover, RNA quantification revealed increased expression of hypertrophy gene markers as atrial natriuretic peptide (ANP), brain natriuretic peptide (BNP), and β-MHC in control mice after TAC as expected. Up-regulation of ANP, BNP, and β-MHC was attenuated upon NF-κB inhibition (*Figure 1C*). Altogether, cardiac-specific inhibition of NF-κB attenuated LV hypertrophy following low-gradient TAC in agreement with the previously described findings concerning attenuation of AngII-induced cardiac hypertrophy by NF-κB inhibition.[7]

We had previously observed male mice to exhibit a more pronounced hypertrophic response than female mice both under chronic AngII stimulation and TAC (data not shown). In order to analyse a possible gender-specific effect of NF-κB inhibition on cardiac hypertrophy, we compared echocardiographic LV wall diameters (IVSd and LVPWd) between

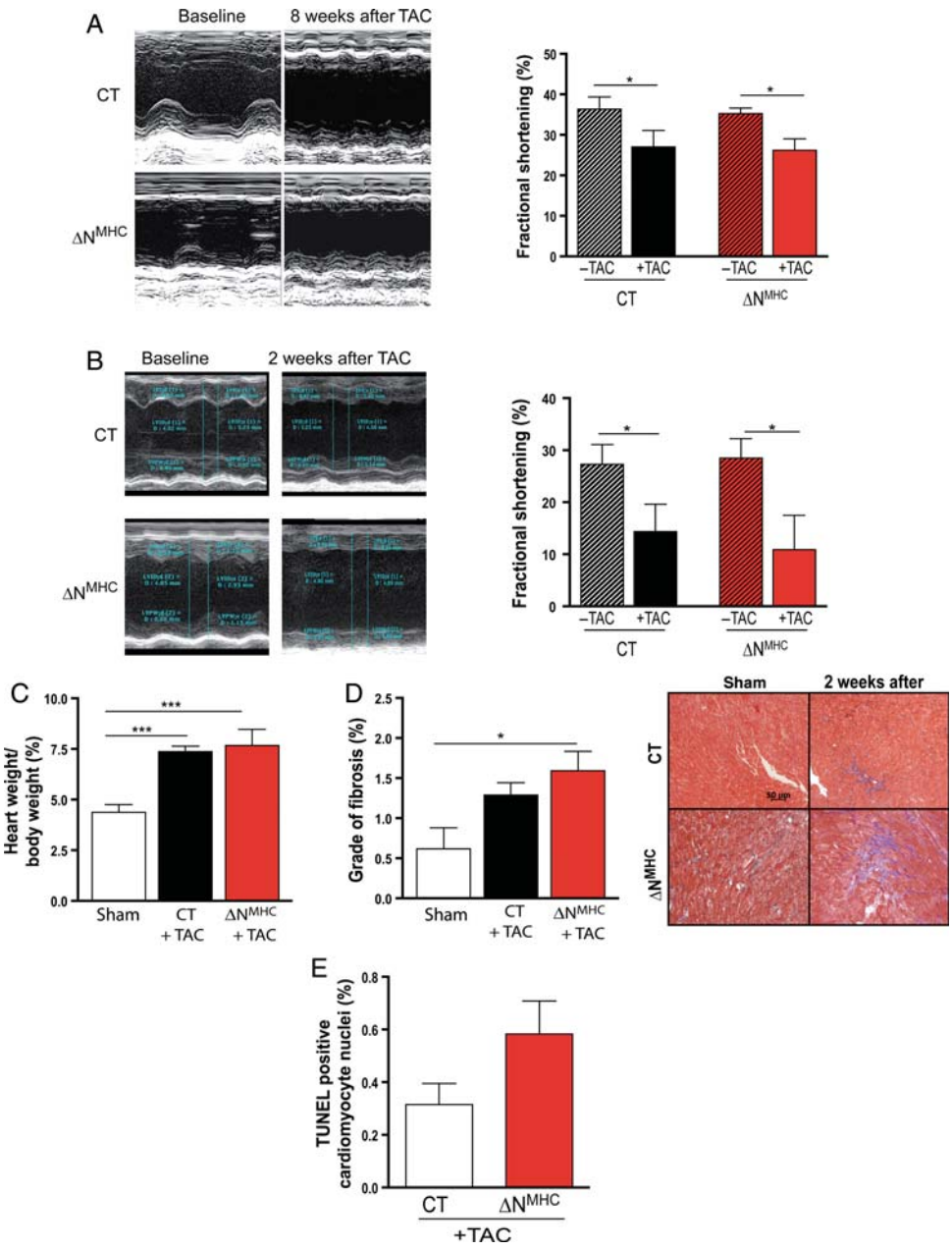

Figure 3 Inhibition of hypertrophy does not translate into attenuated LV remodelling. (*A*) Exemplary echocardiogram of hearts from sham, control, and ΔN^{MHC} mice at baseline and 8 weeks following low-gradient TAC. Quantification of FS from sham, control, or ΔN^{MHC} mice before and after TAC is shown in the bar graph. Despite attenuation of cardiac hypertrophy following TAC in ΔN^{MHC} mice at 4 weeks (*Figure 1*), a deterioration of systolic function as measured by FS is observed. $n = 4$–7 mice per group. (*B*) Representative examples of M-mode echocardiograms and quantification from sham, control, and ΔN^{MHC} mice before and 2 weeks following TAC with high gradient (27 G needle, 48 $\pm$ 4 mmHg gradient). Similar to the low-gradient model, deterioration of FS upon TAC indicating LV remodelling is similar in ΔN^{MHC} and control mice (right bar graph). $n \geq 3$ mice per group. (*C*) Heart-specific NF-κB inhibition upon high-gradient TAC increases cardiac fibrosis. Trichrome staining of cardiac paraffin-embedded sections from sham, control, and ΔN^{MHC} mice after TAC (scale bar = 50 μm). The quantification of the fibrosis-grade shows a significant increase in ΔN^{MHC} mice compared with sham (right bar graph). $^*P < 0.05$, $n = 5$–10 mice per group. (*D*) Quantification of heart/body weight from sham-operated, control, and ΔN^{MHC} mice after TAC with high gradient confirms the observation of significant LV remodelling both in control and ΔN^{MHC} mice at 2 weeks after TAC ($n = 5$–12 mice per group). $^{***}P < 0.001$. (*E*) In association with significant LV remodelling, the number of TUNEL/α-sarcomeric actin/DAPI-positive cardiomyocytes after TAC with high gradient appears to be increased in mice with heart-specific NF-κB inhibition compared with control animals. $n = 5$, $P =$ NS.

male and female mice after low-gradient TAC. Four weeks following TAC, cardiac hypertrophy was significantly blunted only in ΔN^{MHC} male mice as judged by IVSd (CT: 9.0 ± 0.5 vs. ΔN^{MHC}: 6.7 ± 0.7 mm $\times$ 0.1) and LVPWd (CT: 9.6 ± 0.5 vs. ΔN^{MHC}: 7.0 ± 0.04 mm $\times$ 0.1; $P < 0.05$). In contrast, ΔN^{MHC} female mice did not show a difference in LV hypertrophy upon NF-κB inhibition when compared with female controls (*Figure 2* and *Table 1*). Supporting this observation, ΔN^{MHC} male mice exhibited a decrease in heart/body weight ratio (*Table 1*).

3.3 NF-κB inhibition does not prevent LV remodelling

Next, we tested the hypothesis that the attenuation of hypertrophy through NF-κB inhibition would block LV

Table 2 Echocardiography M-mode quantification for ΔN^{MHC} mice at baseline and following high-gradient TAC

TAC with high gradient	Sham, $n = 5$	Control + TAC, $n = 11$	ΔN^{MHC} + TAC, $n = 7$
IVSd (mm × 0.1)			
Before TAC	6.66 ± 0.25	7.37 ± 0.17	7.00 ± 0.24
2 weeks after TAC	8.12 ± 0.54	8.63 ± 0.41	9.28 ± 0.97*
LVPWd (mm × 0.1)			
Before TAC	6.62 ± 0.20	7.33 ± 0.23	7.03 ± 0.24
2 weeks after TAC	7.72 ± 0.48	8.70 ± 0.43	9.68 ± 0.60*
LVDd (mm)			
Before TAC	4.49 ± 0.21	4.05 ± 0.10	4.30 ± 0.11
2 weeks after TAC	4.29 ± 0.35	4.82 ± 0.15	4.54 ± 0.26
FS (%)			
Before TAC	29.69 ± 1.83	27.15 ± 1.78	29.40 ± 2.23
2 weeks after TAC	36.47 ± 3.86	17.91 ± 3.47*	16.84 ± 3.59*
HW/BW (mg/g)	4.42 ± 0.38	7.41 ± 0.29*	7.71 ± 0.81*

Diameters calculated from M-mode of echocardiograms (measurements in mm in diastole) from both control and TG animals following TAC with high gradient (27 G needle). IVSd, inter ventricular septum; LVDd, left ventricular diameter; LVPWd, left ventricle posterior wall dimensions; FS, fractional shortening (%); HW/BW, heart weight/body weight at time of sacrifice. Columns with asterisks are significant compared with sham mice (*$P < 0.05$). $n = 5$–11 for each experiment.

remodelling and prevent the decline in systolic function. To our surprise, M-mode echocardiography tracing demonstrated the decline of fractional shortening (FS), as indicative of systolic function, to be similar at 8 weeks after low-gradient TAC both in controls and in ΔN^{MHC} mice. FS decrease after TAC was shown to be significant in both controls (36.6 ± 3.0 vs. 27.2 ± 4.1%) and ΔN^{MHC} mice (35.5 ± 1.3 vs. 26.3 ± 1.8%, before and 8 weeks after low-gradient TAC, respectively) (*Figure 3A* and *Table 1*).

We reasoned that a more stringent model of cardiac hypertrophy would be required to detect the effect of NF-κB inhibition on LV remodelling. Therefore, we performed TAC with a high gradient (48 ± 4 mmHg). Following 2 weeks of high-gradient TAC, both control and ΔN^{MHC} mice showed significantly reduced FS in comparison to the heart function at baseline (CT: 27.1 ± 1.8 vs. 17.9 ± 3.47% and ΔN^{MHC}: 29.4 ± 2.2 vs. 16.8 ± 3.6% before and 2 weeks after high-gradient TAC, respectively; *Figure 3B* and *Table 2*). ΔN^{MHC} mice exhibited even an exaggerated decrease concerning FS. Furthermore, ΔN^{MHC} animals showed a significantly increased heart/body weight ratio (CT + TAC: 7.4 ± 0.27% and ΔN^{MHC} + TAC: 7.7 ± 0.8% vs. sham: 4.4 ± 0.38; $P < 0.001$) (*Figure 3C*). The reduced FS upon TAC was associated with significantly increased fibrosis in ΔN^{MHC} mice as detected by Masson Trichrome staining in heart sections (*Figure 3D*). Next, we analysed the effect of NF-κB inhibition on cell death following TAC. We found a slightly elevated percentage of TUNEL/α-sarcomeric actin/2′,6′-diamidino-2-phenylindole (DAPI)-positive cells in ΔN^{MHC} mice following TAC in comparison to the controls (*Figure 3E*). In summary, despite ΔN^{MHC} mice attenuated the TAC-induced hypertrophy, LV remodelling was unaffected.

3.4 NF-κB inhibition accelerates AT1-R-induced LV remodelling via enhanced apoptosis and fibrosis

Next, we hypothesized that TAC and AngII might induce LV remodelling via different signalling pathways. We therefore tested the hypothesis that NF-κB inhibition might specifically attenuate AngII-induced cardiac failure. Mice overexpressing the human angiotensin II-receptor (AT1-R) in adult cardiomyocytes under the control of the αMHC promoter (AT1-R-αMHC) demonstrate a phenotype of dilated cardiomyopathy.[9] AT1-Rs were bred to cardiac-specific ΔN^{MHC} mice. Echocardiography demonstrated no significant changes in diameters of IVSd or LVPWd in control mice, AT1-R overexpressing mice, and animals with cardiac-specific double-mutation (ΔN^{MHC} + AT1-R) at baseline and 12 weeks of age (*Figure 4A*). However, RNA quantification revealed increased expression of the hypertrophy gene markers ANP, BNP, β-MHC, and α-sarcomeric actin when comparing both TG mice (AT1-$R^{\alpha MHC}$ and ΔN^{MHC}+ AT1-R) and controls (*Figure 4B*). Both AT1-R and ΔN^{MHC}+ AT1-R mice exhibited a marked reduction of FS in comparison to controls (CT: 29.7 ± 4.1%, AT1-$R^{\alpha MHC}$: 16.7 ± 1.7%, and ΔN^{MHC}+ AT1-R: 13.9 ± 5.0%; $P < 0.05$) (*Figure 4C*). Quantification of TUNEL/α-sarcomeric actin/DAPI-positive cells demonstrated significantly increased cardiomyocyte apoptosis in ΔN^{MHC}+ AT1-R mice in comparison to controls, whereas AT1-$R^{\alpha MHC}$ mice showed a slight increase when compared with control mice (*Figure 4D*). In addition, the grade of fibrosis assessed by Masson Trichrome staining was also increased in double-mutated mice compared with both AT1-$R^{\alpha MHC}$ ($P < 0.01$) and controls ($P < 0.05$) (*Figure 4E*). To confirm that IκBα repressor overexpression and therefore NFκB inactivation are consistent in the different stress models, we analysed IκBα expression and p65 acetylation, which indicates the transcriptional activity of p65 in the nucleus and consequent NFκB signalling activation. As demonstrated by QRT-PCR, IκBα RNA was significantly less expressed in AT1-$R^{\alpha MHC}$ in comparison to ΔN^{MHC} mice as expected; however, the expression of IκBα in ΔN^{MHC}+ AT1-R double-mutants was increased in comparison to AT1-$R^{\alpha MHC}$ single transgenes (*Figure 4F*). Moreover, acetylation of p65 was remarkably less in ΔN^{MHC} mice when compared with controls, indicating successful repression of p65 to translocate into the nucleus, where the acetylation event takes place. Acetylation of p65 in AT1-$R^{\alpha MHC}$ animals was confirmed to be up-regulated, consistent with the NF κB activation upon hypertrophic stimuli. However, p65 acetylation was down-regulated in ΔN^{MHC}+ AT1-R mice in

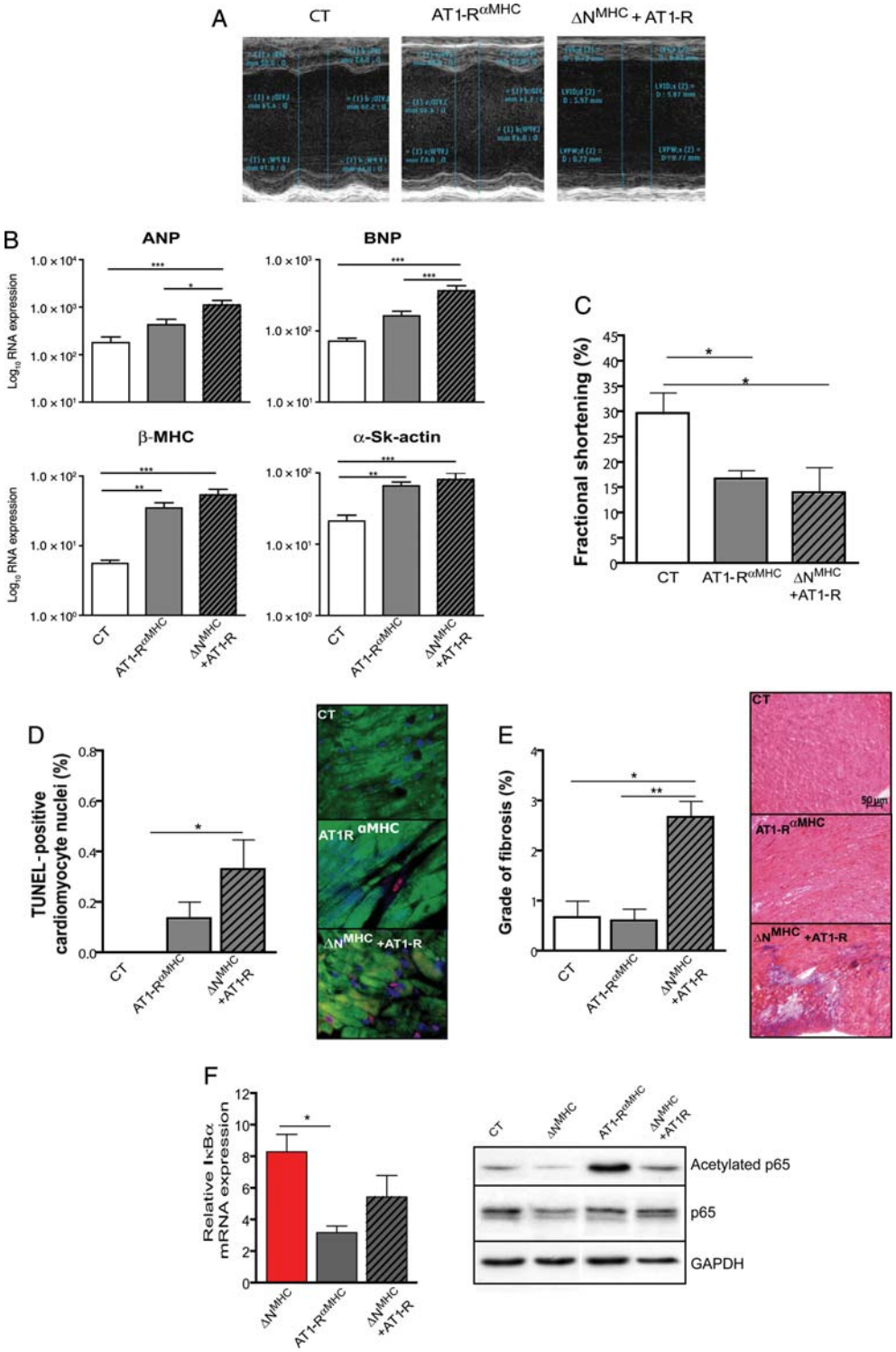

Figure 4 NF-κB inhibition accelerates AngII-induced heart failure. Phenotype of mice expressing the human AT1-R under the control of the αMHC promoter cross-bred to ΔN^{MHC} mice. (*A*) Representative examples of M-mode echocardiograms of hearts from controls, AT1-R$^{\alpha MHC}$, and ΔN^{MHC}+ AT1-R mice at baseline. (*B*) RNA quantification by real-time RT–PCR analysis of hypertrophic markers ANP, BNP, β-MHC, and α-Skactin in controls, AT1-R$^{\alpha MHC}$, and ΔN^{MHC}+ AT1-R mice at 12 weeks of age. NF-κB inhibition aggravates the hypertrophic phenotype with significantly higher gene expression of ANP and BNP when compared with AT1-R$^{\alpha MHC}$ mice. (*C*) No attenuation of LV remodelling in AT1-R$^{\alpha MHC}$ mice upon NF-κB inhibition as determined by severe impairment of FS in ΔN^{MHC}+ AT1-R mice. (*D*) Aggravation of LV remodelling by NF-κB inhibition in association with enhanced cardiomyocyte apoptosis and (*E*) significantly enhanced fibrosis in ΔN^{MHC}+ AT1-R mice compared with control and AT1-R$^{\alpha MHC}$ mice. (*F*) NF-κB-dependent gene transcriptional inactivation in ΔN^{MHC}+ AT1-R demonstrated by QRT-PCR of IκBα expression, which is significantly up-regulated when compared with single AT1-R$^{\alpha MHC}$ mice. Acetylation of p65, indicative of NF-κB transcriptional activation, is decreased in ΔN^{MHC} in comparison to controls as well as in ΔN^{MHC}+ AT1-R when compared with single AT1-R$^{\alpha MHC}$ mutants, as demonstrated by western blot analysis. $^{*}P < 0.05$, $^{**}P < 0.01$, $^{***}P < 0.001$; $n = 4$ mice per group for western blot analysis and $n = 4$–9 for RT–PCR quantification.

comparison to single AT1-R$^{\alpha MHC}$ mutants, indicating successfully NF-κB inhibition in the double-mutants (*Figure 4F*). In summary, NF κB inhibition aggravates LV remodelling following chronic renin–angiotensin system stimulation through increased cardiomyocyte apoptosis and cardiac fibrosis.

4. Discussion

This study tested the hypothesis whether inhibition of cardiac hypertrophy through genetic blockade of NF-κB activity in αMHC^{pos} cardiomyocytes abrogates LV remodelling upon chronic pressure overload or increased AngII signalling. Cardiac hypertrophy upon TAC was attenuated in male mice with NF-κB inhibition; NF-κB inhibition had no significant effect on cardiac hypertrophy in female mice. However, despite initially attenuation of LV hypertrophy upon NF-κB inhibition, systolic LV function declined in response to pressure overload. The lack of effect on LV remodelling was not stimulus-specific, as NF-κB inhibition even increased tissue fibrosis and LV dilation in a genetic AngII-dependent heart failure model based on cardiac AT1-R overexpression. These data suggest NF-κB to be part of the adaptive hypertrophy-signalling cascade specifically in male mice, which is required to maintain systolic function upon stress.

Some studies suggest that blocking LV hypertrophy is sufficient to attenuate LV dilation and loss of FS,[3] whereas other studies find even progressive LV remodelling despite inhibition of LV hypertrophy.[11] This discrepancy might be explained by certain pathways mediating exclusively 'adaptive' hypertrophy in the sense of LV function preservation.[2] In contrast, signals mediating mal-adaptive hypertrophy induce a progressive decline in LV function and may serve as valuable drug targets. Our data suggest NF-κB to be part of the adaptive hypertrophy signalling in male mice, since its blockade had no positive—and in part even detrimental—effect on LV remodelling in chronic pressure overload. The data highlight the importance of analysing every hypertrophy mediator also concerning its effect on global LV remodelling, since the paradigm of inhibiting hypertrophy being sufficient to attenuate LV remodelling appears to be questionable.

We also analysed the effect of NF-κB inhibition on a different genetic model of AngII-induced cardiomyopathy. Mice constitutively overexpressing the AT1-R under the control of the αMHC promoter develop a dilated cardiomyopathy phenotype rapidly over a few weeks after birth.[9,13] NF-κB inhibition accelerated progression of LV remodelling with significantly increased cardiomyocyte apoptosis. We previously found a similar effect of NF-κB *in vitro*.[7] The requirement of NF-κB for cardiac hypertrophy and its role as a survival factor allows the assessment of the relative importance of both cardiomyocyte hypertrophy and apoptosis for global LV remodelling. As hypertrophied cardiomyocytes are more susceptible to apoptosis,[14] inhibition of hypertrophy was regarded to be sufficient to block LV remodelling. Our data support the notion that both events occur in parallel and the inhibition of hypertrophy—at least through attenuation of NF-κB activation—is not sufficient to block the deleterious effect of increased cardiomyocyte apoptosis in LV remodelling.

Our initial data and previous studies indicated male mice to exhibit more pronounced cardiac hypertrophy upon pressure overload. In this study, we found NF-κB inhibition specifically attenuating cardiac hypertrophy in male ΔN^{MHC} mice, whereas female mutants exhibited the same extent of cardiac hypertrophy as their controls. Anti-androgen treatment of female hypertensive rats attenuated end-organ damage;[15] this observation suggests a deleterious effect of androgens in LV remodelling. The present data suggest the NF-κB pathway to be relevant for the gender differences observed upon TAC and other models of chronic pressure overload.

In summary, we found NF-κB activity to be beneficial in cardiac hypertrophy induced by either chronic pressure overload or increased cardiac angiotensin receptor signalling in male mice. Inhibition of NF-κB attenuates the initial hypertrophy but does not protect against progressive LV remodelling. We conclude LV hypertrophy and remodelling to be dissociated concerning some signalling pathways like the NF-κB, which may be critical for adaptive vs. mal-adaptive hypertrophic response.

Acknowledgements

The authors acknowledge superb technical assistance from Bärbel Pohl and Martin Taube. We thank R. Schmidt-Ullrich and C. Scheidereit (Max Delbrück Center for Molecular Medicine) for providing floxed IκBα mice and M. Schneider (Imperial College, London) for providing αMHC-Cre mice. AT1-R$^{\alpha MHC}$ mice were kindly provided by P. Paradis and M. Nemer, Montréal, Canada.

Conflict of interest: none declared.

Funding

This study was funded by Grimmke Stiftung and Juergen Manchot Stiftung (to M.W.B.) and an MDC Research Grant to M.W.B.

References

1. McKinsey TA, Kass DA. Small-molecule therapies for cardiac hypertrophy: moving beneath the cell surface. *Nat Rev Drug Discov* 2007;**6**:617–635.
2. Dorn GW 2nd. The fuzzy logic of physiological cardiac hypertrophy. *Hypertension* 2007;**49**:962–970.
3. Esposito G, Rapacciuolo A, Naga Prasad SV, Takaoka H, Thomas SA, Koch WJ *et al*. Genetic alterations that inhibit in vivo pressure-overload hypertrophy prevent cardiac dysfunction despite increased wall stress. *Circulation* 2002;**105**:85–92.
4. Skavdahl M, Steenbergen C, Clark J, Myers P, Demianenko T, Mao L *et al*. Estrogen receptor-beta mediates male-female differences in the development of pressure overload hypertrophy. *Am J Physiol Heart Circ Physiol* 2005;**288**:H469–H476.
5. Gerdts E, Okin PM, de Simone G, Cramariuc D, Wachtell K, Boman K *et al*. Gender differences in left ventricular structure and function during antihypertensive treatment: the Losartan Intervention for Endpoint Reduction in Hypertension Study. *Hypertension* 2008;**51**:1109–1114.
6. Freshour JR, Chase SE, Vikstrom KL. Gender differences in cardiac ACE expression are normalized in androgen-deprived male mice. *Am J Physiol Heart Circ Physiol* 2002;**283**:H1997–H2003.
7. Freund C, Schmidt-Ullrich R, Baurand A, Dunger S, Schneider W, Loser P *et al*. Requirement of nuclear factor-kappaB in angiotensin II- and isoproterenol-induced cardiac hypertrophy in vivo. *Circulation* 2005; **111**:2319–2325.
8. Schmidt-Ullrich R, Aebischer T, Hulsken J, Birchmeier W, Klemm U, Scheidereit C. Requirement of NF-kappaB/Rel for the development of hair follicles and other epidermal appendices. *Development (Cambridge, England)* 2001;**128**:3843–3853.
9. Paradis P, Dali-Youcef N, Paradis FW, Thibault G, Nemer M. Overexpression of angiotensin II type I receptor in cardiomyocytes induces cardiac hypertrophy and remodeling. *Proc Natl Acad Sci USA* 2000;**97**:931–936.

10. van Empel VP, Bertrand AT, van Oort RJ, van der Nagel R, Engelen M, van Rijen HV *et al*. EUK-8, a superoxide dismutase and catalase mimetic, reduces cardiac oxidative stress and ameliorates pressure overload-induced heart failure in the harlequin mouse mutant. *J Am Coll Cardiol* 2006;**48**:824–832.
11. Baurand A, Zelarayan L, Betney R, Gehrke C, Dunger S, Noack C *et al*. Beta-catenin downregulation is required for adaptive cardiac remodeling. *Circ Res* 2007;**100**:1353–1362.
12. Krappmann D, Wulczyn FG, Scheidereit C. Different mechanisms control signal-induced degradation and basal turnover of the NF-kappaB inhibitor IkappaB alpha in vivo. *EMBO J* 1996;**15**:6716–6726.
13. Harris IS, Zhang S, Treskov I, Kovacs A, Weinheimer C, Muslin AJ. Raf-1 kinase is required for cardiac hypertrophy and cardiomyocyte survival in response to pressure overload. *Circulation* 2004;**110**: 718–723.
14. Kang PM, Yue P, Liu Z, Tarnavski O, Bodyak N, Izumo S. Alterations in apoptosis regulatory factors during hypertrophy and heart failure. *Am J Physiol Heart Circ Physiol* 2004;**287**:H72–H80.
15. Baltatu O, Cayla C, Iliescu R, Andreev D, Bader M. Abolition of end-organ damage by antiandrogen treatment in female hypertensive transgenic rats. *Hypertension* 2003;**41**:830–833.